Title
Internal temperature measurements in response to cryogen spray cooling of a skin phantom

Authors
Torres, Jorge H
Anvari, Bahman
Tanenbaum, BS
et al.

Publication Date
1999-06-22

DOI
10.1117/12.350956

Internal temperature measurements in response to cryogen spray cooling of a skin phantom

Jorge H. Torres[a], Bahman Anvari[a], B. Samuel Tanenbaum[b], Thomas E. Milner[c], Jason C. Yu[b], J. Stuart Nelson[d]

[a] Department of Bioengineering, Rice University, Houston, TX 77005
[b] Department of Engineering, Harvey Mudd College, Claremont, CA, 91711
[c] Biomedical Engineering Program, University of Texas at Austin, Austin, TX 78712
[d] Beckman Laser Institute and Medical Clinic, University of California Irvine, CA, 92612

ABSTRACT

Cryogen spray cooling (CSC) can protect the epidermis from non-specific thermal injury during laser treatment of port wine stains and other hypervascular cutaneous malformations. Knowledge of skin internal temperatures in response to CSC is essential for optimization of this technique. We used an epoxy resin compound to construct a skin phantom and measured its internal temperatures in response to cooling with different cryogens at various spurt durations, spraying distances, and ambient humidity levels. The measured temperature distributions during CSC were fitted by a mathematical model based on thermal diffusion theory.

For spurt durations up to 100 ms, temperature reduction within the phantom remained confined to the upper 200 μm, and was affected by spraying distance. Depending on the cryogen used, temperature reductions up to 45 °C could be measured 20 μm below the surface at the end of a 100 ms spurt. However, the cryogen film temperature on the epoxy resin surface was up to 35 °C lower, indicating lack of perfect thermal contact at the cryogen film-phantom interface. Theoretical predictions were within 10% of measured temperatures. Ice formation occurred following termination of the spurt and was influenced by the ambient humidity level.

Keywords: cutaneous hypervascular malformations, lasers, refrigerants, heat transfer, skin model, dermatology.

1. INTRODUCTION

It has been demonstrated that cryogen spray cooling (CSC) can protect the epidermis from non-specific thermal injury during laser treatment of port wine stains (PWS) and other hypervascular cutaneous malformations while still allowing photocoagulation of targeted blood vessels [1-4]. Further development and optimization of this technique requires knowledge of internal skin temperatures as CSC parameters are varied.

Inasmuch as direct measurement of skin internal temperatures (e.g., via thermal microsensors) is difficult to implement, indirect but reliable methods have to be used. One such method involves the use of a phantom with thermal properties similar to those of skin. Furthermore, a physically stable, non-degradable phantom provides a medium in which the effects of various CSC parameters can be studied.

We investigated the effects of cryogen type, spurt duration, spraying distance, and ambient humidity level on the internal temperature distribution in an epoxy resin phantom. The experimental results obtained while utilizing the phantom were subsequently used in conjunction with a mathematical model based on diffusion theory to predict temperature distributions within human skin.

JHT (Correspondence): E-mail: jhtorres@ruf.rice.edu; Telephone: (713)527-8101x3027; Fax: (713)737-5877

Part of the SPIE Conference on Cutaneous Applications of Lasers: Dermatology, Plastic Surgery, and Tissue Welding • San Jose, California • January 1999
SPIE Vol. 3590 • 0277-786X/99/$10.00

2. THEORY

We assume a semi-infinite medium is cooled by spraying its surface with a liquid cryogen. Since the lateral dimensions of the cooled surface (≈ 1 - 1.5 cm in practice) are much larger than the thickness of the medium (≈ 1 mm), temperature distribution may be computed by solving the one-dimensional heat conduction equation:

$$\frac{\partial^2 T(z>0,t>0)}{\partial z^2} = \frac{1}{\alpha}\frac{\partial T(z,t>0)}{\partial t} \tag{1}$$

where T ($z > 0$, $t > 0$) (°C) is the medium temperature in response to CSC (beginning at t=0), z (m) is distance into the medium (with origin at the medium surface), t (s) is time, and α ($m^2 \bullet s^{-1}$) is the medium thermal diffusivity (either for the skin or for the epoxy resin).

A Robin boundary condition at the medium surface is implemented:

$$-k\frac{\partial T(z,t>0)}{\partial z}\bigg|_{z=0} = h\left[T_\infty - T(0,t>0)\right] \tag{2}$$

where k ($W \bullet m^{-1} \bullet K^{-1}$) is the thermal conductivity, T_∞ (°C) is the temperature of the cryogen film in contact with the target surface during a spurt, and h ($W \bullet m^{-2} \bullet K^{-1}$) is the average heat transfer coefficient at the cryogen film-medium interface. As $h \rightarrow \infty$, thermal resistance at the cryogen-medium interface diminishes and perfect thermal contact between the two media is achieved; conversely, as $h \rightarrow 0$, resistance becomes infinite and the surface is a perfect insulator.

Solution to equation (1) with boundary condition (2) is [5]:

$$T(z,t>0) = (T_i - T_\infty)\left[\mathrm{erf}(\tilde{z}) + \exp(-\tilde{z}^2)\,\mathrm{erfcx}(\tilde{z}+\tilde{h})\right] + T_\infty \tag{3}$$

where,

$$\mathrm{erfcx}(x) = \exp(x^2)\,\mathrm{erfc}(x) \quad , \tag{4a}$$

$$\tilde{h} = \frac{h\sqrt{\alpha t}}{k} \quad , \tag{4b}$$

$$\tilde{z} = \frac{z}{2\sqrt{\alpha t}} \quad . \tag{4c}$$

In the above expressions, T_i is medium initial temperature prior to CSC, and erfc (x) is the complementary error function (1-erf(x)). Since both T_∞ and h are unknown, their values are determined from experimental measurements (section 4).

3. MATERIALS AND METHODS

3.1 Internal Temperature Measurements in an Epoxy Resin Phantom

An epoxy resin compound (EP30, Master Bond Inc., Hackensack, NJ) was used to construct a skin phantom. The manufacturer's reported value for the thermal diffusivity of the epoxy resin was $0.7 \bullet 10^{-7}$ $m^2 \bullet s^{-1}$, within 36% of that for skin ($1.1 \bullet 10^{-7}$ $m^2 \bullet s^{-1}$ [6]). We confirmed the thermal diffusivity value of the epoxy resin by means of a technique that utilizes self heated thermistors [7]. Additionally, we measured the epoxy heat capacity by using a standard dual scanning calorimetry technique.

Four K-type thermocouples (Chromega-Alumega®, Omega Engineering, Inc., Stamford, CT), with a wire diameter of 12.7 μm and a sensing bead of 30 μm were used for temperature measurements. The thermocouples were carefully positioned and fixed on a thin epoxy resin slab under direct visualization through a dissecting microscope. The slab with attached thermocouples was later placed in a specially constructed Teflon® mold which was filled with the liquid epoxy resin. Following a 72 hour curing period, a 6 x 6 x 4 cm solid epoxy block with four embedded thermocouples was formed. The positions of the thermocouples, as measured from the epoxy resin front surface to the bead centers, were: 20, 90, 200,

and 400 μm (Figure 1). The uncertainty in thermocouple positions due to microscope measurement error was ±5 μm. In addition to the four embedded subsurface thermocouples, a fifth thermocouple (same type and size) was placed on the epoxy resin phantom surface to measure cryogen film temperature. When sprayed directly with a cryogen spurt, the response time of the thermocouples (to 67%) was 1.5 - 2 ms, with a nearly 100% response in 3 ms.

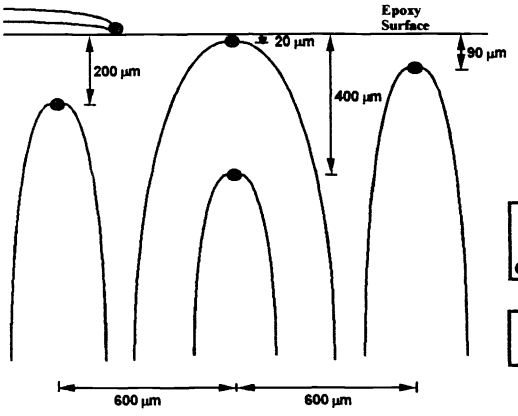

Figure 1. Micro-thermocouple placement within epoxy resin phantom. One micro-thermocouple was placed over the phantom surface.

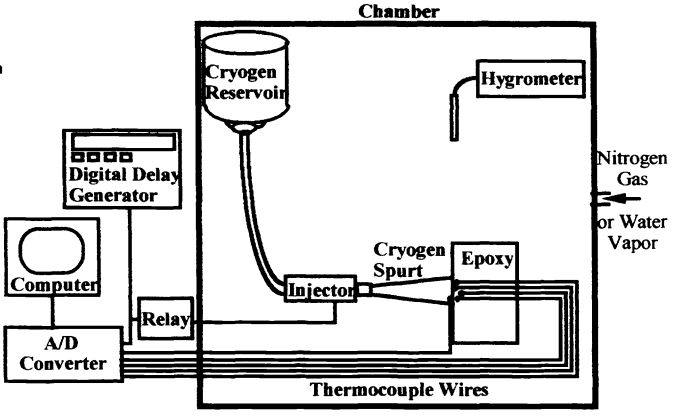

Figure 2. Schematics of the instrumentation used for internal temperature measurements in the epoxy resin phantom in response to CSC.

The thermocouple wires were connected to an external 14 bit A/D converter (instruNet Direct-Sensor-to-Data Acquisition system, Omega Engineering Inc., Stamford, CT) and a PCI controller card plugged into a computer. The system software was set to a sampling rate of 1 kHz for each of the six input channels used (five for the thermocouples and one for the injector trigger signal).

3.2 Cryogen Spray Cooling of the Epoxy Resin Phantom

Cryogens 134a (1,1,1,2 Tetrafluoroethane; National Refrigerants, Inc., Rosenhayn, NJ) (boiling point≈ -26°C at 1 atm), 404a (Forane®, a mixture of Tetrafluoroethane, Trifluoroethane and Pentafluoroethane; ELF Atochem North America, Inc., Philadelphia, PA) (boiling point ≈ - 48°C at 1 atm), and 407c (a mixture of Tetrafluoroethane, Pentafluoroethane and Difluoromethane; ICI KLea, Wilmington, DE) (boiling point ≈ - 43°C at 1 atm), environmentally compatible, non-toxic, chloro-fluorocarbon substitutes [8-10] were used as cooling agents. Each cryogen, contained in a pressurized steel canister, was sprayed through an electronically controlled standard automobile fuel injection valve (Figure 2) over the phantom surface from a distance varying from 5 - 100 mm. The resulting diameter of the cooled site on the epoxy resin phantom was approximately 10 - 15 mm. Both the injector and the phantom were placed in a sealed plexiglass® chamber. Relative humidity in the chamber was controlled by filling it with either dry nitrogen gas or water vapor. Experiments were performed at 8, 50, and 98% relative humidity levels. The relative humidity inside the chamber was measured by a digital thermo-hygrometer (Model RH 411, Omega Engineering, Inc., Stamford, CT). The cryogen spurt duration τ varied from 20 to 100 ms and was controlled by a programmable digital delay generator (DG535, Stanford Research Systems, Sunnyvale, CA). Internal epoxy resin temperatures in response to CSC were measured as described in section 3.1 and fitted by the mathematical model described in section 2 to estimate the unknown heat transfer coefficient h at the cryogen film-phantom interface.

4. RESULTS

An example of measured temperatures within the epoxy resin phantom in response to a 100 ms R-134a spurt sprayed from 60 mm distance at 50% relative humidity is shown in Figure 3a. The cryogen film

temperature measured by the thermocouple placed on the surface was approximately -44°C during the spurt, well below the cryogen boiling point of -26°C, an indication that further cooling of cryogen droplets takes place as they travel from the injector towards the phantom surface. The temperature 20 μm below the epoxy resin surface only reached -14°C at the end of the spurt, 30°C above the cryogen film temperature. Liquid cryogen remained on the thermocouple placed over the surface of the epoxy for 700 ms following termination of the spurt. The surface temperature plateau at approximately 0°C corresponds to melting of ice formed over the phantom. An expanded view of Figure 3a is presented in Figure 3b to show only the internal temperatures measured during the 100 ms spurt. Temperature reductions immediately upon termination of a 100 ms spurt were 39, 19, and 4°C at 20, 90, and 200 μm below the surface, respectively. No temperature reduction was measured 400 μm below the surface.

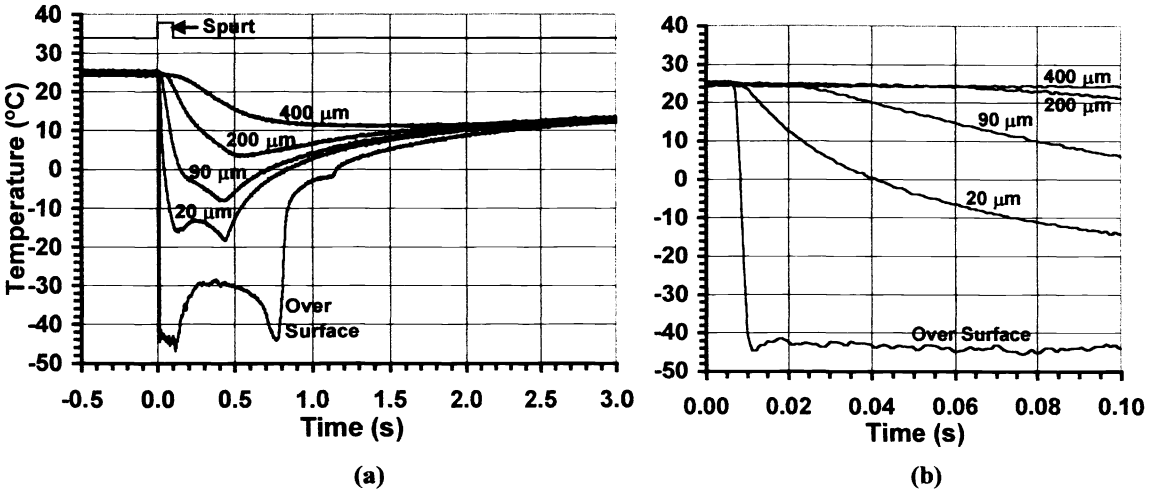

Figure 3. **(a)** Example of epoxy phantom internal temperature measurements in response to CSC with R-134a. Spurt duration: 100 ms; Spraying distance: 60 mm. **(b)** Expansion of (a) to show the temperatures during the 100 ms spurt.

Figure 4 shows temperature histories at a depth of 20 μm in response to 60 ms spurts with the three cryogens used in the study. Since R-404a and R-407c have lower boiling points than R-134a, lower temperatures were induced within the epoxy resin phantom in response to cooling with these cryogens.

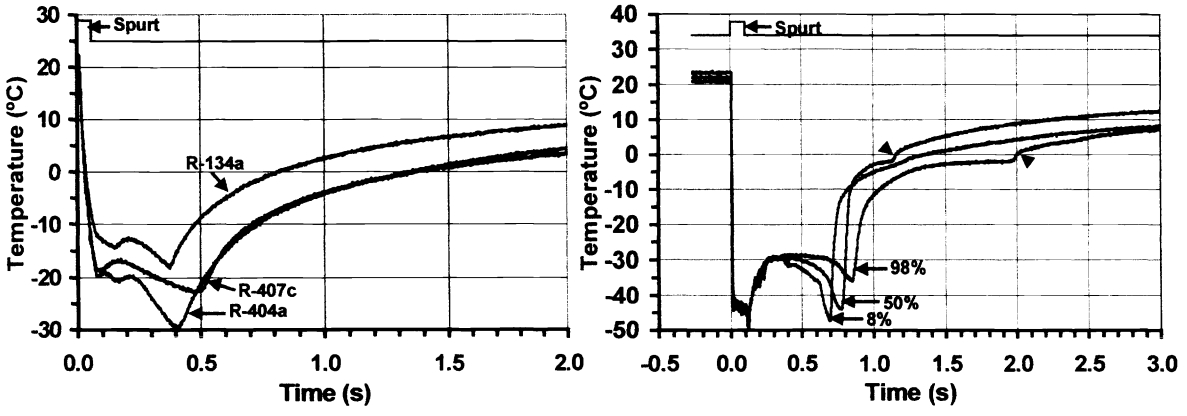

Figure 4. Measured temperatures at 20 μm during CSC of epoxy phantom with three cryogens: R-134a, R-404a, and R-407c. Spurt duration: 60 ms; Spraying distance: 60 mm.

Figure 5. Temperature measured on the phantom surface during CSC with cryogen R-134a for three ambient relative humidity levels.

Temperature measurements on the phantom surface are presented in Figure 5 for three relative humidity levels. Ice was formed on the surface following termination of the spurt. As evidenced by the broadening of the temperature plateau at approximately 0°C, the amount of ice formation at the surface increased with increasing ambient relative humidity level. The transitions at 0°C are indicated in the figure by the small arrows for the 50 and 98% humidity levels. Changes in the ambient humidity level did not influence the cryogen film temperature (first 300 ms). Following termination of the spurt (after 100 ms), the film temperature returned to -29°C regardless of the ambient humidity level.

Figure 6 summarizes the effects of spraying distance and relative humidity level on the temperature of the cryogen film over the phantom surface. The bars in the diagram extend from an initial temperature of 20°C to the temperature attained at the end of 20, 60, and 100 ms spurts with cryogen 134a at various spraying distances and relative humidity levels. The cryogen film temperature decreases with increasing spraying distance as progressively cooler droplets arrive at the target surface due to further evaporation in flight. At 5 mm, the cryogen film temperature is -29°C, close to the boiling point (-26°C). At 100 mm, a temperature of 48-50°C is measured. Varying the spurt duration or the ambient humidity level does not change the cryogen film temperature by more than 5% for a given spraying distance.

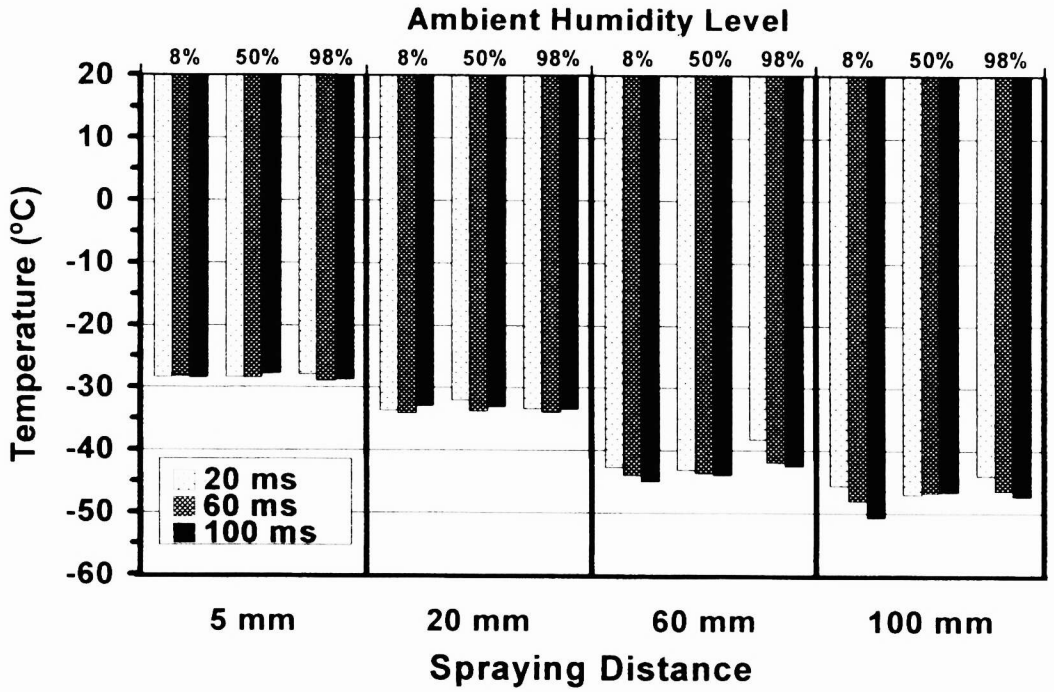

Figure 6. Temperature of the cryogen R-134a film over the phantom surface for various spraying distances, spurt durations, and ambient humidity levels.

Internal temperature reductions at 20, 90, and 200 μm within the epoxy resin phantom upon termination of 20, 60, and 100 ms spurts are summarized in Figures 7a and 7b for cryogens R-134a and R-404a, respectively. For 60 and 100 ms spurts, temperature reduction at depths of 20 and 90 μm increased with increasing spraying distance up to 60 mm. For a 20 ms spurt, increasing the spraying distance did not significantly affect the temperature reductions up to 60 mm. The small temperature reductions at 200 μm were not affected by the spraying distance. For all three spurt durations, temperature reductions decreased when the spraying distance was increased from 60 to 100 mm. Depending on the type of cryogen used, respective maximum temperature reductions at 20, 90, and 200 μm were 39-46°C, 19-23°C, and 3-4°C, at the end of 100 ms spurt. No temperature reduction was observed at a depth of 400 μm, and therefore it is not shown. Internal temperatures were not affected by the ambient relative humidity level.

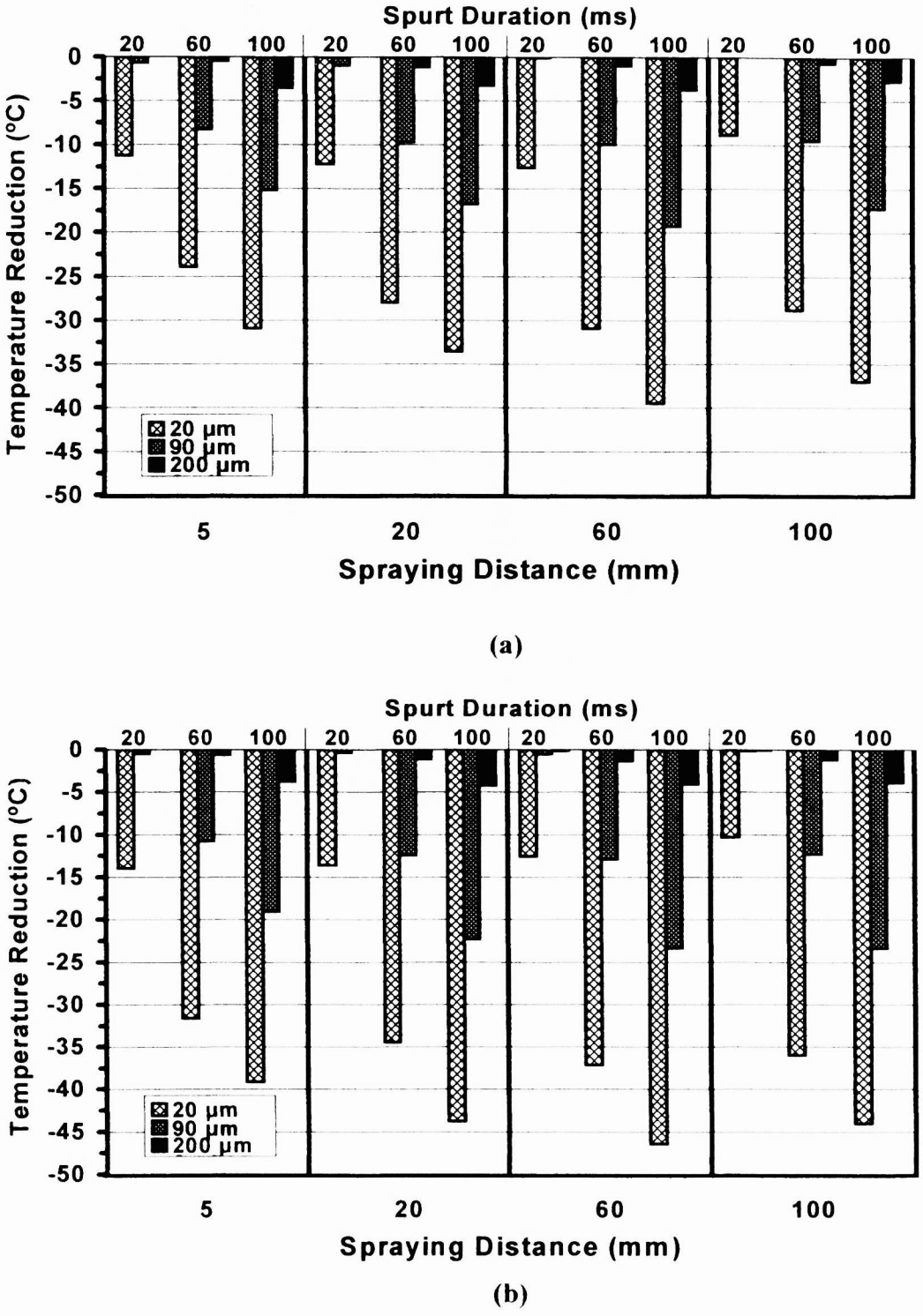

Figure 7. Internal temperature reductions at three depths within the epoxy resin phantom in response to CSC with **(a)** R-134a, and **(b)** R-404a, for various spraying distances and spurt durations.

Cryogen film temperature, T_∞, during the spurt was –44°C at a distance of 60 mm based on the measurements obtained with the thermocouple placed over the phantom surface. This value was used in the theoretical model to compute internal temperature distributions.

Computed and measured temperatures within the epoxy resin in response to a 100 ms R-134a spurt are presented in Figure 8. Temperatures were computed at depths within ±5 μm of the thermocouple bead centers, and the best fit with the experimental measurements within that range was used. Inasmuch as there was no temperature reduction at a depth of 400 μm during the spurt, no temperature curves are presented for this depth; however, the computed temperature curve at the surface is shown. By fitting the measured temperature curve at 20 μm depth, the surface heat transfer coefficient (h) at the cryogen film-epoxy resin interface was estimated to be 2,400 $W \cdot m^{-2} \cdot K^{-1}$. Using the same h value, excellent agreement (within 5-10%) was obtained between predicted and measured temperatures at depths of 90, 200 and 400 μm. Similar agreement between predicted and measured temperatures was found for the other cryogens. For cryogen 404a, in particular, a film temperature of -63°C was measured and an h value of 2,300 $W \cdot m^{-2} \cdot K^{-1}$ was estimated following the same procedure described above. The h values reported here are consistent with values determined by radiometric surface measurements performed on PWS patients [11].

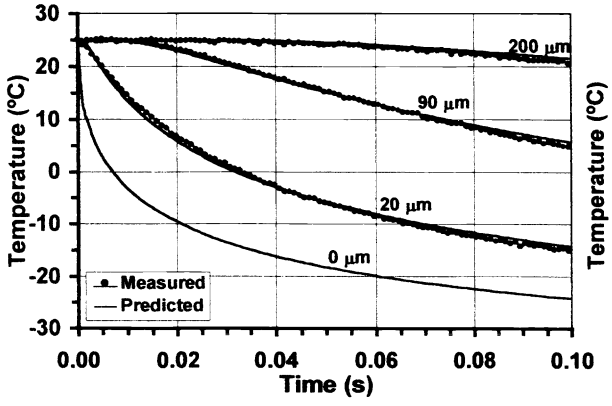

Figure 8. Theoretical vs measured internal temperatures in epoxy resin phantom in response to a 100 ms R-134a spurt. Spraying distance: 60 mm.

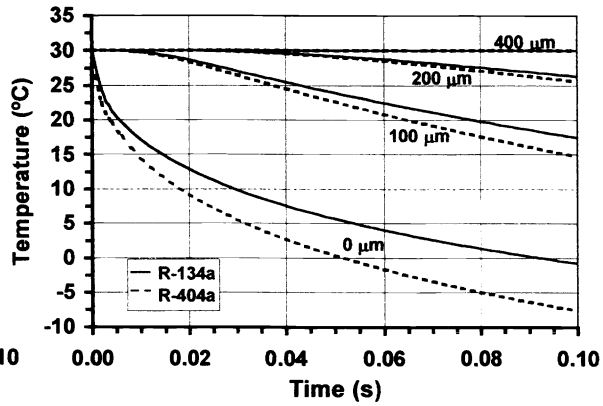

Figure 9. Predicted internal temperatures in human skin in response to 100 ms R-134a and R-404a spurts.

Internal temperatures in human skin in response to CSC are computed by using the reported thermal diffusivity for skin ($1.1 \cdot 10^{-7}$ $m^2 \cdot s^{-1}$ [8]) in the thermal diffusion model. Predicted temperatures at 0, 100, 200, and 400 μm depths in response to 100 ms R-134a and R-404a spurts are presented in Figure 9. Depending on the cryogen, temperature reductions of 31-38°C at the surface, 12-15°C at a depth of 100 μm, and 4-5°C at a depth of 200 μm are predicted for human skin, at the end of the spurt. No temperature reduction is predicted at a depth of 400 μm for either cryogen.

5. DISCUSSION

Knowledge of internal skin temperatures in response to CSC is essential for optimization of this technique and improvement in treatment outcome for patients with PWS and other cutaneous hypervascular malformations undergoing laser therapy in conjunction with CSC. An epoxy resin compound has been used in this study as skin phantom. The phantom allowed controlled positioning of micro-thermocouples and provided a stable, reproducible medium for testing of various cooling parameters. In this phantom, the effects of cryogen type, spurt duration, spraying distance, and ambient humidity level have been investigated.

Measured cryogen film temperatures on the phantom surface are well below the corresponding cryogen boiling point. Cryogen droplets cool significantly as a result of evaporation while in flight from the injector to the phantom surface. Consequently, the cryogen film temperature over the surface decreases

with increasing spraying distance up to 60 mm. Neither the spurt duration nor the ambient humidity level has appreciable influence on the cryogen film temperature. Lower temperature of the cryogen film accounts for the progressively lower temperatures measured internally in the epoxy phantom as the spraying distance is increased. However, beyond a 60 mm spraying distance, the amount of liquid cryogen reaching the target is greatly reduced due to excessive in-flight droplet evaporation, resulting in less effective cooling of the target. There is an optimal spraying distance for maximum cooling effect. This optimal distance is likely to depend on the size and number of the droplets generated by a specific atomizer (injector).

The ambient humidity level does not have a significant effect on the target temperatures during the cryogen spurt application. However, there is an effect on the amount of ice formation on the target surface following termination of the spurt. Based on visual inspection during CSC of epoxy phantom and other substrates, the ice forms over target surface immediately after the cryogen film has completely evaporated. Temperature transitions due to melting of ice occur at 0°C, and a temperature plateau just below 0°C increases with increasing relative humidity. However, based on Figures 3a and 4, ice formation at the surface does not seem to have a significant impact on the subsurface temperatures. The above observations on the effects of spraying distance and humidity level are consistent with our previous report in which human skin was cooled under various conditions [12].

Depending on the type of cryogen used, internal temperature measurements in the epoxy resin phantom show maximum temperature reductions of 39-46°C at a depth of 20 μm, 19-23°C at 90 μm, and 3-4°C at 200 μm at the end of a 100 ms spurt and for a 60 mm spraying distance. The larger temperature reductions correspond to CSC with R-404a. Although 7°C additional cooling is obtained at 20 μm with the use of R-404a when compared with R-134a, the temperature difference is only 4°C at 90 μm and decreases with depth. No temperature reduction was observed at a depth of 400 μm with either cryogen.

Before any prediction of skin internal temperatures can be made, the surface heat transfer coefficient during CSC must be determined. Temperature measurements of the cryogen film over the epoxy resin surface and at a depth of 20 μm within the epoxy resin show a considerable temperature difference that indicates poor thermal contact (low heat transfer coefficient, h , on the order of 2,300-2,400 $W \cdot m^{-2} \cdot K^{-1}$) at the cryogen film-epoxy interface. A vapor layer between liquid cryogen film and a "hot" substrate surface (e.g., skin or epoxy resin phantom) may be partially responsible for such poor thermal contact. The presence of a vapor layer has been reported for liquids sprayed onto a hot surface [13,14].

Temperatures predicted by the heat transfer model agree within a few percent with those measured by the thermocouples positioned in the epoxy resin at depths of 90, 200, and 400 μm. Using the skin thermal diffusivity in the mathematical model, temperature reductions of 31°C at the surface, 12°C at a depth of 100 μm, and 4°C at 200 μm are predicted for human skin at the end of a 100 ms R-134a spurt. No temperature reduction is predicted at a depth of 400 μm. Confinement of the cooling effect to the upper 200 μm of the skin allows selective epidermal protection during laser treatment of cutaneous vascular malformations. In patients with port wine stains, abnormal vessels are usually located at depths ≥ 200 μm [15]. CSC utilizing R-404a provides additional temperature reduction (≈ 7°C at the surface) when compared to those with R-134a, but the additional cooling effect rapidly decreases with depth (3°C difference at 100 μm) (Figure 9). For either cryogen, further cooling of the epidermis may be achieved, in theory, if the thermal contact at the cryogen film-skin interface could be improved (i.e., h could be increased). We are currently investigating methods to improve thermal contact to optimize clinical application of CSC

6. CONCLUSIONS

We have utilized an epoxy resin phantom to quantify the internal temperature distribution in response to CSC. At the surface, cryogen film temperature is lower than the cryogen boiling point and progressively decreases, up to a limiting value, as the spraying distance is increased. The film temperature is not affected by spurt duration nor ambient humidity level. However, following termination of the spurt, increased ice formation on the target surface is observed with increasing ambient humidity. During CSC, a high thermal resistance (low h) is present at the cryogen film-medium interface. Internal temperatures in the epoxy resin phantom are successfully fitted with a mathematical model based on

simple thermal diffusion theory. Computed internal skin temperatures indicate that localized cooling within 300 μm is achieved.

ACKNOWLEDGMENTS

The authors wish to thank Lih-Huei Liaw for her invaluable technical support throughout the experiments, Qing Liu and Rudolf K. Meszlenyi for their assistance with heat capacity measurements of the epoxy resin, Naresh C. Bhavaraju for performing thermal conductivity and diffusivity measurements on the epoxy resin, and Sol Kimel for helpful discussions on cryogen thermodynamics.

This work was supported in part by The Whitaker Foundation Biomedical Engineering Research (95-21025, 96-0235) and Special Opportunity Grants, the National Science Foundation (BES-9896101), Institute of Heart, Lung and Blood (IR15-HL581215-01, HL59472-03), Institute of Arthritis and Musculoskeletal and Skin Disease (AR43419) at the National Institutes of Health.

REFERENCES

1. J. S. Nelson, T. E. Milner, B. Anvari, B. S. Tanenbaum, S. Kimel, L. O. Svaasand "Dynamic epidermal cooling during pulsed laser treatment of port wine stains: a new methodology with preliminary clinical evaluation," *Arch. Dermatol.*, vol. 131, pp. 695-700, 1995.
2. J. S. Nelson, T. E. Milner, B. Anvari, B. S. Tanenbaum, L. O. Svaasand, and S. Kimel, "Dynamic epidermal cooling in conjunction with laser-induced photothermolysis of port wine stain blood vessels," *Lasers Surg. Med.*, vol. 19, pp. 224-229, 1996.
3. E. J. Fiskerstrand, L. T. Norvang, and L. O. Svaasand, "Laser treatment of port wine stains; reduced pain and shorter duration of purpura by epidermal cooling," SPIE Proc., vol. 2922, pp. 20-28, 1996.
4. H. A. Waldorf, T. S. Alster, K. McMillan, A. N. B. Kauvar, R. G. Geronemus, J. S. Nelson, "Effect of dynamic cooling on 585-nm pulse dye laser treatment of port-wine stain birthmarks," *Derm. Surg.*, vol. 23, pp. 657-662, 1997.
5. H. S. Carslaw, and J. C. Jaeger, *Conduction of Heat in Solids. 2nd edn.* Oxford: Clarendon Press, 1959.
6. F. A. Duck, *Physical Properties of Tissue. A Comprehensive Reference Book.* London: Academic Press, 1990.
7. J. W. Valvano, J. R. Cochran, and K. R. Diller, "Thermal conductivity and diffusivity of biomaterials measured with self heated thermistors," *Int. J. Thermophysics.*, vol. 6, pp. 301-311, 1985.
8. L. E. Manzer, "The CFC-ozone issue: progress on the development of alternatives to CFCs," *Science*, vol. 249, pp. 31-35, 1990.
9. D. J. Alexander, and S. E. Libretto, "An overview of the toxicology of HFA-134a (1,1,1,2-tetrafluoroethane)," *Hum. Exp. Toxicol.*, vol. 14, pp. 715-720, 1995.
10. W. Dekant, "Toxicology of chlorofluorocarbon replacements," *Environ. Health Perspect.*, vol. 104, supp. 1, pp. 75-83, 1996.
11. J. H. Torres, J. S. Nelson, B. S. Tanenbaum, T. E. Milner, D. M. Goodman, and B. Anvari, "Estimation of internal skin temperatures in response to cryogen spray cooling: implications for laser therapy of port wine stains," *IEEE J. Special Topics Quant. Elect.*, in review.
12. B. Anvari, B. J. Ver Steeg, T. E. Milner, B. S. Tanenbaum, T. J. Klein, E. Gerstner, S. Kimel, and J. S. Nelson, "Cryogen spray cooling of human skin: effects of ambient humidity level, spraying distance, and cryogen boiling point," *SPIE Proc.*, vol. 3192, pp. 106-110, 1997.
13. W. M. Grissom, and F. A. Wierum, "Liquid spray cooling of a heated surface," *Int. J. Heat Mass Transfer*, vol. 24, pp. 261-271, 1981.
14. T. Y. Xiong, and M. C. Yuen, "Evaporation of a liquid droplet on a hot plate," *Int. J. Heat Mass Transfer*, vol. 34, pp. 1881-1894, 1991.
15. S. H. Barsky, S. Rosen, D. E. Geer, and J. M. Noe, "The nature and evolution of port wine stains: A computer assisted study," *J. Invest. Dermatol.*, vol. 74, pp. 154-157, 1980.